Lipophilic Salirasib analogs with enhanced antiproliferative activity against human solid tumor cell lines.

Exequiel O. J. Porta,[a] María Sol Ballari,[a] José M. Padrón,[b] and Guillermo R. Labadie*[,a,c]

a. Instituto de Química Rosario (IQUIR), Universidad Nacional de Rosario-CONICET, Suipacha 531, S2002LRK, Rosario, Argentina.

b. BioLab, Instituto Universitario de Bio-Orgánica “Antonio González” (IUBO-AG), Universidad de La Laguna, Apartado 456, E-38071, La Laguna, Spain

c. Departamento de Química Orgánica, Facultad de Ciencias Bioquímicas y Farmacéuticas, Universidad Nacional de Rosario, Rosario, Argentina.

*Corresponding author: Tel.: +54-341-4370477; e-mail: labadie@iquir-conicet.gov.ar.

Abstract:

Aim: We proposed to determine the antiproliferative activity of a series of synthetic salirasib analogs, presenting or not a 1,2,3-triazole linker, against five different cancer cell lines. **Results**: Bioassay, cheminformatic, and *in silico* ADME-Tox allowed the identification of new potent analogs. SAR analysis allowed the identification of structural and physicochemical features that benefit the antiproliferative activity. **Conclusion**: Isoprenyl R chains with three or more isoprene units, or long aliphatic R chains are the preferred ones within the active compounds. Likewise, we have identified three compounds with better activity profiles than salirasib against all the cell lines tested.

Graphical abstract:

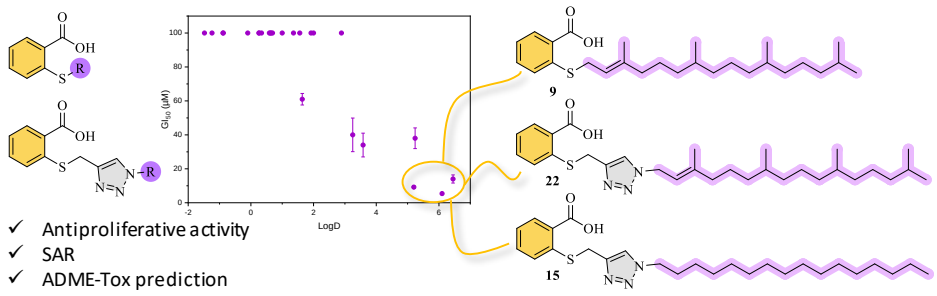

Keywords: Salirasib; 1,2,3-triazoles; Cancer; SAR studies; Cheminformatics.

Introduction

Cancer is a large group of diseases that can start in almost any organ or tissue of the body when abnormal cells grow uncontrollably, and is the second leading cause of death globally [1]. Guanine binding proteins (G proteins) such as Ras, Rap, Rho, and Rab enclose the largest group of isoprenylated proteins. Among these, Ras proteins have attracted particular attention because of the important role they play in carcinogenesis [2]. These proteins are engaged in signal transduction pathways, crucial for cell growing and differentiation. Specific mutations in Ras proteins turn them into oncogenic and they are found in around 30% of all human tumors, including near 90% of pancreatic cancers and 50% of colon cancers [3].

Ras proteins undergo prenylation in a three-step post-translational process that facilitates membrane association to Ras, a crucial step to trigger its oncogenic activity [4]. In the first step of prenylation, which occurs in the cytoplasm, an isoprenyl transferase (Farnesyl Transferase, FTase, or Geranylgeranyl Transferase, GGTase) recognizes a carboxyl terminus CAAX motif of Ras (C: Cisteine, AA: two aliphatic amino acids, X: a final varied amino acid), and a farnesyl (FTase) or geranylgeranyl (GGTase) group is transferred to the cysteine of CAAX, forming a thioether bond with the corresponding sulphydryl group. After prenylation, the protein can migrate to the endoplasmic reticulum, where a Ras Converting CAAX Endopeptidase 1 (RCE-1) cleaves the -AAX tail, leaving the C-terminus with an isoprenylcysteine. This motif is recognized by Isoprenylcysteine Carboxymethyl Transferase (ICMT), which catalyzes the transfer of a methyl group from an *S*-adenosyl-L-methionine to the isoprenylated Ras terminus carboxylate to form an esther, allowing the membrane anchoring of Ras [2,5].

The development of anticancer agents through a Ras-related mechanism has been approached by different strategies. One alternative is to directly prepare Ras inhibitors, such as DABP-GTP [6] (**Fig. 1**), a GTP analog, or by an anti-sense RNA like ISIS 2503 [7], which has undergone clinical trials in various cancer types. A strategy that has gained relevance over the years is the development of inhibitors for the post-translational prenylation process at any of its three stages. FTase inhibitors have been successful in pre-clinical studies [8,9], but many of them failed in phase III of clinical trials, because many Ras mutants (e.g, KRAS, NRAS, etc.) proved to be good GGTase substrates when FTase is inhibited [4,10]. However, FTase inhibitor clinical trials for Ras mutants

that did not show this effect are promising [11,12]. Inhibition of RCE-1 was also studied [13–15], but experiments in mice have thrown discouraging results [16,17], and this target was set aside. ICMT inhibitors have gained relevance among the Ras-dependent anti-cancer agents [5]. Amid ICMT inhibitors, the most relevant are the indole cysmethynil [18] and the substrate analog salirasib [19,20] (**Fig. 1**).

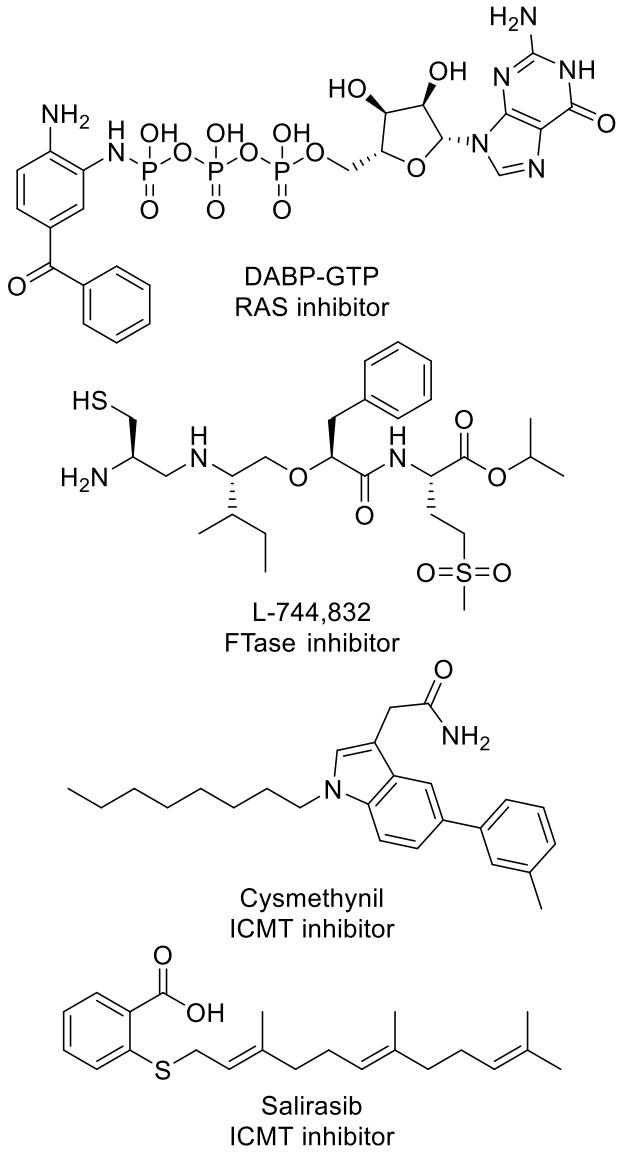

Fig. 1. RAS-related anti-cancer agents.

Salirasib, or farnesylthiosalicylic acid (FTS), is a salicylic acid derivative with antineoplastic activity. It was designed as a competitor of *S*-farnesyl cysteine on Ras [21–23], and it acts as a potent competitive inhibitor of ICMT. In consequence, salirasib selectively disrupts the association of activated Ras proteins to the plasma membrane [24,25]. This compound is usually indicated for the treatment of a wide range of cancers, such as

pancreas, lung, and colon, among others. Preclinical and phase I clinical trials in Ras-positive cancer patients showed that salirasib could be well tolerated, with no significant side effects and with the predicted levels of absorption [26–28]. There is still little information about phase II clinical trials, which at least required dosage increments to improve results [29]. Hence, the scientific community is still working on salirasib structural optimization that could lead to improve the late stages of clinical trials [30–34].

We have previously reported the synthesis and antimalarial activity of salirasib analogs as a mean of drug repurposing [35]. The compounds collection consists on thiosalicylic acid (TSA) derivatives, *S*-substituted with alkyl, propargyl, ester, aryl or isoprenyl chains (**1** - **13**), or with a triazole linker inserted between the TSA and the R substituent (**14** - **25**) (**Fig. 2**). In this opportunity, we present the results of the salirasib analogs as antiproliferative agents, along with their SAR and predicted ADME-Tox analysis.

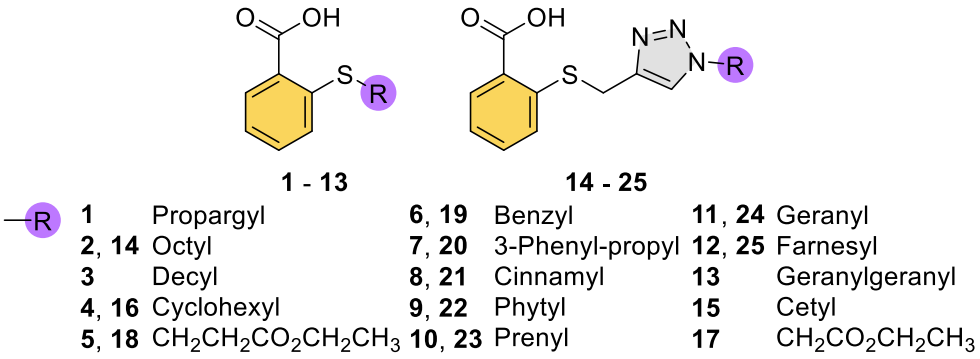

Fig. 2. Salirasib analogs studied in this work.

Materials and Methods

General method for the preparation of S-alkylated thiosalicylic acid compounds

Thiosalicylic acid (1 equivalent) was dissolved in anhydrous acetone (10 mL/eq), under constant stirring and inert atmosphere. Next, guanidinium carbonate (1 equivalent) and organobromide compound (1 equivalent) were added. The reaction mixture was brought to reflux for 8 hours. To finish the reaction, a solution of 1M HCl was added, continuing to extract the compound of interest with ethyl ether (3 x 25 mL). Combined organic extracts were dried with sodium sulfate and evaporated. Products **1** - **13** were purified by column chromatography in silica gel with increasing hexanes/ethyl acetate gradients.

General procedure for the Cu(I) mediated 1,3-dipolar cycloaddition (CuAAC)

Alkyne **1** (1 equivalent) and azide (1.5 equivalent) were suspended in 10 mL/eq of tBuOH:H_2O (1:1). Then, 1 M CuSO4 solution (0.05 equivalents) and 1 M sodium ascorbate solution (0.2 equivalents) were added, and the mixture stirred overnight at room temperature. Brine (30 mL) was added and the solution was extracted with dichloromethane (3 x 25 mL). Combined organic extracts were dried over sodium sulfate and evaporated. Products **14** – **25** were purified by column chromatography in silica gel with increasing hexane/ethyl acetate gradients.

General procedure for in vitro antiproliferative activity

The *in vitro* antiproliferative activity of investigated compounds was evaluated using the protocol of the National Cancer Institute of the United States [36]. A panel of five human solid tumor cell lines was used:

- A549: adenocarcinomic human alveolar basal epithelial cells, extracted from cancerous lung tissue in the explanted tumor of a 58 years old caucasian male (non-small cell lung cancer);
- SW1573: alveolar cell carcinoma extracted from a 44 years old white female (non-small cell lung cancer);
- HeLa: cervical cancer cells extracted from Henrietta Lacks, a 31 years old African-American female (cervix cancer);
- HBL-100: extracted from the milk of a 27 years old caucasian nursing mother and obtained 3 days after delivery (breast cancer);
- T-47D: isolated from a pleural effusion obtained from a 54 years old female patient with an infiltrating ductal carcinoma of the breast (breast cancer).

Cells were maintained in 25 cm 2 culture flasks in RPMI 1640 supplemented with 5% heat-inactivated fetal calf serum, and 2 mM L-glutamine in a 37 ºC, 5% CO_2, 95% humidified air incubator. Exponentially growing cells were trypsinized and re-suspended in antibiotic-containing medium (100 units penicillin G and 0.1 mg of streptomycin per mL). Single-cell suspensions displaying > 97% viability by trypan blue dye exclusion were subsequently counted. After counting, dilutions were made to give the appropriate cell densities for inoculation onto 96-well microtiter plates. Cells were inoculated in a volume of 100 µL per well at densities of 2500 (A549,

HBL-100, HeLa and SW1573) or 5000 (T-47D) cells per well, based on their doubling times. Compounds to be tested were dissolved in DMSO at an initial concentration of 40 mM. Control cells were exposed to an equivalent concentration of DMSO (0.25% v/v, negative control). Each compound was tested in triplicate at different dilutions in the range 1–100 µM. The drug treatment was started on day 1 after plating. Drug incubation times were 48 h, after which time cells were precipitated with 25 µL ice-cold TCA (50% w/v) and fixed for 60 min at 4 ºC. Then the sulforhodamine B (SRB) assay was performed [37]. The optical density (OD) of each well was measured at 530 nm, using BioTek's PowerWave XS Absorbance Microplate Reader. Values were corrected for background OD from wells only containing medium. Antiproliferative activity of the compounds was expressed as GI_{50}, that is, the concentration of the compound that inhibits 50% of the culture growth.

Physicochemical properties prediction

Using Osiris DataWarrior platform [38], a search in ChemBL database [39,40] was made. Filters on target (ICMT), Organism (*Homo sapiens*), and inhibitory activity (< 100 µM) were applied. This search thrown a total on 467 reported *Hs*ICMT inhibitors. On the same platform, relevant properties were predicted (Total Molweight, cLogP, cLogS, and Total Surface Area). Also on Osiris DataWarrior platform, SMILES of the 25 farnesylthiosalicylic acid (FTS) analogues were introduced, and the same properties were predicted. For the FTS analogues, LogD was also predicted, using the online ChemAxon LogD predictor [41].

ADMETox predictions

Computational modelling to estimate the bioavailability, aqueous solubility, human intestinal absorption, metabolism, mutagenicity, toxicity, etc. for the compounds was performed using the SwissADME [42], pkCSM [43] and Biotransformer [44] platforms.

SwissADME: The SMILES of compounds **1** - **25** were uploaded to SwissADME (http://www.swissadme.ch/), pasting the list of smiles on the designated window. The following parameters were calculated: *Physicochemical Properties* (Formula, MW, Num. heavy atoms, Num. arom. heavy atoms, Fraction Csp3, Num. rotatable bonds, Num. H-bond acceptors, Num. H-bond donors, Molar Refractivity and TPSA); *Lipophilicity* (Log Po/w (iLOGP), Log Po/w (XLOGP3), Log Po/w (WLOGP), Log Po/w (MLOGP), Log Po/w (SILICOS-IT) and Consensus Log Po/w); *Water Solubility* (Log S (ESOL), Solubility, Class, Log S (Ali), Solubility, Class, Log S (SILICOS-IT),

Solubility and Class); *Pharmacokinetics* (GI absorption, BBB permeant, P-gp substrate, CYP1A2 inhibitor, CYP2C19 inhibitor, CYP2C9 inhibitor, CYP2D6 inhibitor, CYP3A4 inhibitor and Log Kp -skin permeation-); *Druglikeness* (Lipinski, Ghose, Veber, Egan, Muegge and Bioavailability Score); *Medicinal Chemistry* (PAINS, Brenk, Lead likeness and Synthetic accessibility).

pkCSM: The SMILES of compounds **1** - **25** were uploaded to pkCSM (http://biosig.unimelb.edu.au/pkcsm/prediction), through a *.txt SMILE file. The following parameters were calculated: *Absorption* (Water solubility, Caco2 permeability, Intestinal absorption (human), Skin Permeability, P-glycoprotein substrate, P-glycoprotein I inhibitor, P-glycoprotein II inhibitor); *Distribution* (VDss (human), Fraction unbound (human), BBB permeability, CNS permeability); *Metabolism* (CYP2D6 substrate, CYP3A4 substrate, CYP1A2 inhibitior, CYP2C19 inhibitior, CYP2C9 inhibitior, CYP2D6 inhibitior, CYP3A4 inhibitior); *Excretion* (Total Clearance, Renal OCT2 substrate); *Toxicity* (AMES toxicity, Max. tolerated dose (human), hERG I inhibitor, hERG II inhibitor, Oral Rat Acute Toxicity (LD50), Oral Rat Chronic Toxicity (LOAEL), Hepatotoxicity, Skin Sensitisation, *T.Pyriformis* toxicity, Minnow toxicity).

Biotransformer: The SMILES of compounds **9**, **12**, **13**, **14**, **15**, **22** and **25** were uploaded to Biotransformer (http://biotransformer.ca/). The metabolites prediction was performed for one-step CYP450 catalyzed reactions.

Results and discussion

The salirasib analogs **1** - **13** were easily obtained from thiosalicylic acid and the proper halide in the presence of guanidinium carbonate in refluxing acetone, and compounds **14** – **25** were obtained through Click chemistry between propargyl thiosalicylic acid **1** and the proper azide, as we have previously reported [35]. The different R substituents were chosen in order to fill a wide place in chemical space, producing compounds with structural diversity and with an appropriate physicochemical properties distribution.

Since our compounds were inspired in salirasib, an ICMT inhibitor, we decided to compare the physicochemical properties of our compound collection with reported ICMT inhibitors. A search in ChemBL database [39,40] afforded a total of 467 reported *Hs*ICMT inhibitors. Using Osiris DataWarrior platform [38], we calculated the physicochemical properties of the ChemBL database and our collection. Normalized histograms are shown in **Fig. 3**, where molecular weight (MW), total surface area, cLogP and cLogS are presented,

comparing the distribution of the different properties among compounds belonging to the ChemBL database and our set of salirasib analogs. We can observe that the property distributions are very similar between both sets. For the ChemBL database, the maximum compound counts were at MW = 350 – 400 Da, total surface area = 250 – 300 Å^2, cLogP = 4.5 – 5, and cLogS = -5 – (-4.5). Instead, for our set of compounds, maximum counts were at MW = 250 - 350 Da, total surface area = 200 – 250 Å^2, cLogP = 3 – 3.5, and cLogS = -4.5 – (-4). The most frequent values for each property were a bit lower for our salirasib analogs library, but overall our collection covers a wide range of desirable properties to afford a good antiproliferative activity against cancer cell lines.

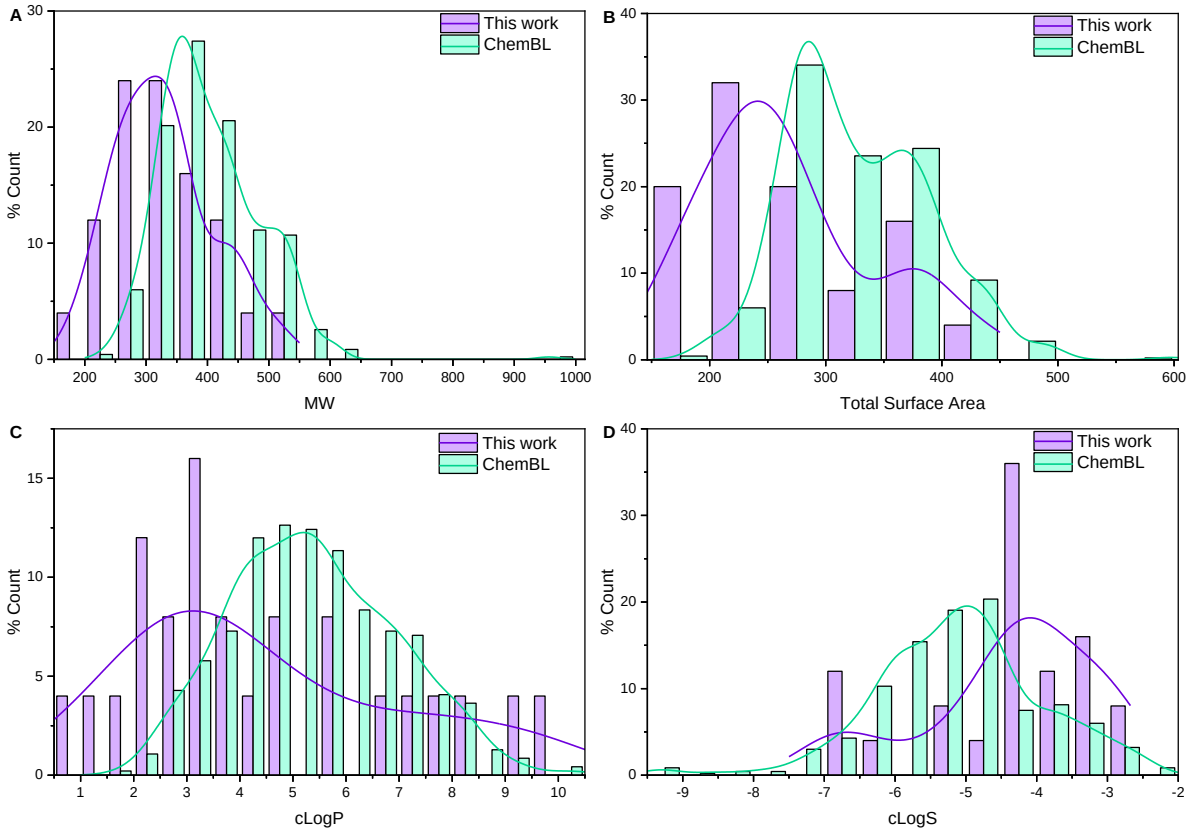

Fig. 3. Normalized physicochemical properties distribution for ChemBL dataset (ChemBL, green bars) and Salirasib analogs dataset (This Work, violet bars). Distributions were fitted to Kernel Smooth function (green and violet lines for ChemBL and This Work datasets, respectively). A) MW; B) Total Surface Area; C) cLogP; D) cLogS.

The *in vitro* antiproliferative activity of compounds **1** - **25** were tested against a panel of five human solid tumor cell lines: A549 (non-small cell lung), HeLa (cervix), SW1573 (non-small cell lung), T-47D (breast), and HBL-100 (breast) [45]. The measurement of the corresponding GI_{50} was carried out, and results are shown in **Table 1**.

GI_{50} is defined as the half maximal inhibitory concentration. The compounds were tested at a maximum concentration of 100 μM. Seven of the twenty-five compounds assayed were active against the five cell lines (GI_{50} < 100 μM), and showed a similar trend against all of them. The detailed analysis of the **Table 1**, excluding Salirasib that is considered the positive control, showed only six compounds have GI_{50} below 100 mM. The GI_{50} of the active analogs are around 40 μM for the less potent, to below 5 μM for the most effective, without substantial differences between the cell lines.

Table 1. Antiproliferative activity of salirasib and its analogs (GI_{50} < 100 μM).

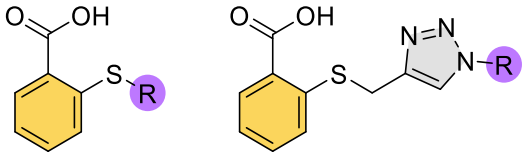

1 - 13 **14 - 25**

Compound	Family	R	GI_{50} (μM) A549	HeLa	SW1573	T-47D	HBL-100	GI_{50} range plot
9	*S*-R	Phytyl	14 ± 2.4	12 ± 2.4	15 ± 3.3	18 ± 1.3	14 ± 1.9	
12	*S*-R	Farnesyl (Salirasib)	34 ± 7.0	34 ± 5.1	41 ± 10	42 ± 9.3	22 ± 5.4	
13	*S*-R	Geranylgeranyl	38 ± 6.1	29 ± 2.9	37 ± 6.7	41 ± 0.6	23 ± 1.8	
14	*S*-triazolyl-R	Octyl	61 ± 3.4	39 ± 6.5	47 ± 7.9	93 ± 11	40. ± 0.3	
15	*S*-triazolyl-R	Cetyl	9.2 ± 0.7	6.9 ± 0.04	9.3 ± 0.03	20 ± 5.9	14 ± 1.2	
22	*S*-triazolyl-R	Phytyl	5.4 ± 0.7	4.3 ± 1.3	5.8 ± 0.6	9.6 ± 1.3	10 ± 1.1	
25	*S*-triazolyl-R	Farnesyl	40 ± 9.9	33 ± 3.3	40 ± 6.3	52 ± 11	33 ± 0.9	

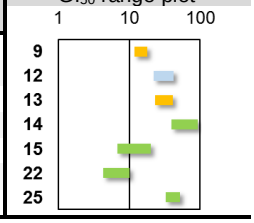

Values are mean ± standard deviation of two to three independent experiments.

All the active compounds have in common that the sulphur is bound to an electron deficient carbon. So, the presence of an allyl or 4-triazolyl methylene next to the sulphur could be playing an important role in the recurrence of antiproliferative activity, but it would not be the only requirement. It was also very interesting to note that all the active analogs present long lipophilic chain substitutions, with or without a triazole linker, of at least eight carbon atoms. The most preferred R chains are farnesyl, geranylgeranyl, phytyl and cetyl. Interestingly, phytyl (**9**, **22**) and cetyl (**15**) analogs, are both 16 carbons long, were more active than salirasib (**12**), as deduced from the GI_{50} range plot (Table 1). This indicates that the R chain would be occupying the farnesyl pocket in the ICMT. Probably, the more flexible cetyl and phytyl chains could accommodate better in the lipophilic cavity, producing an activity increment.

In particular, compound **22** is the hit of this collection and has been shown to have better antiproliferative activity in all cell lines tested: it is 6.3 times more active in A549, 8 times more active in HeLa, 7 times more active in SW1573, 4.4 times more active in T-47D, and 2.2 more active in HBL-100 compared with salirasib. **Fig. 4** shows the activity profile of all active compounds, and their comparison with salirasib. It results interesting that

the thiosalicylic acid *S*-substituted with a triazolyl phytyl group presented the best performance. Phytyl *S*-substitution was previously studied in cysteine analogs, achieving interesting results as non steroidal anti inflamatory agents targeting ICMT [46–49]. Also, in our previous study of salirasib analogs as antimalarial agents, phytyl substituted compounds, both with or without the triazole linker, were the most active compounds of the series, and presented similar potencies as the observed on the tumor cell lines (**9**, IC_{50} (*P. falciparum*) = 13.40 ± 1.53 µM; **22**, IC_{50} (*P. falciparum*) = 9.75 ± 1.97 µM) [35]. This reinforces our hypothesis, where the triazolyl-phytyl group could be considered as a privileged structure for ICMT inhibitors, enhancing the thiosalicylic acid interaction with the active site. To our knowledge, the triazolyl-isoprenyl *S*-substitution of cysteine analogs was not previously studied as antiproliferative agents.

	A549	HeLa	SW1573	T-47D	HBL-100
9	▲ 2.43	▲ 2.83	▲ 2.73	▲ 2.33	▲ 0.64
12	▬ 1.00	▬ 1.00	▬ 1.00	▬ 1.00	▬ 1.00
13	▼ 0.89	▲ 1.17	▲ 1.11	▲ 1.02	▼ 1.05
14	▼ 0.56	▼ 0.87	▼ 0.87	▼ 0.45	▼ 1.82
15	▲ 3.70	▲ 4.93	▲ 4.41	▲ 2.10	▲ 0.64
22	▲ 6.30	▲ 7.91	▲ 7.07	▲ 4.38	▲ 0.45
25	▼ 0.85	▲ 1.03	▲ 1.03	▼ 0.81	▼ 1.50

Fig 4. Trend map of active compounds against tumor cell lines (A549, HeLa, SW1573, T-47D, HBL-100). The green triangles show an improvement in biological activity compared to salirasib, while the red triangles show a loss of activity. The numbers reflect the improvement or loss of activity (= GI_{50}salirasib / GI_{50}product).

In order to have a deeper insight of the physicochemical properties required for this collection (and its biological response), we graphed different properties vs GI_{50} for each cell line: MW, total surface area, LogD, and cLogS. Similar trends were observed for all the cell lines, so SAR graphs for A549 cell line were chosen to represent the panel (**Fig. 5**), while graphs for the rest can be found in the Supporting Information. Since our compounds collection have ionizable groups that are charged at physiological pH, LogD (pH = 7) [41] results a better lipophilicity descriptor than cLogP, and the former was used in the SAR analysis. It can be observed that there is a clear “high activity” zone for each property. In fact, there is a preference for active compounds that present a MW > 350 Daltons, total surface area > 300 $Å^2$, LogD > 3, and cLogS < -5.

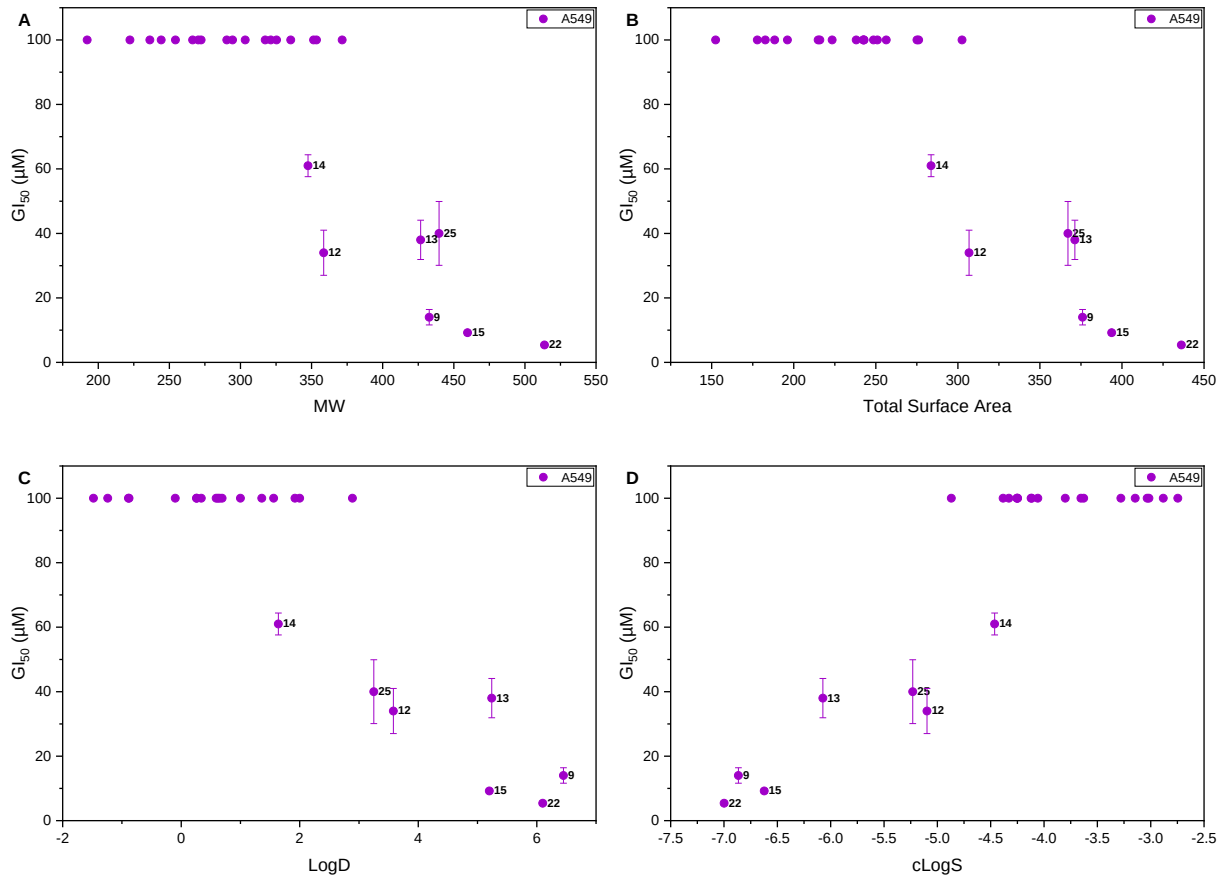

Fig. 5. Correlation between antiproliferative activity against A549 cell line and physicochemical properties. A) MW; B) Total Surface Area; C) LogD; D) cLogS.

Additionally, looking to predict the potential of the compounds as leads and their ADME-Tox properties, the selected candidates were evaluated using the web-based software SwissADME [42], Biotransformer [44] and pkCSM [43] (See Supporting Information). The SwissADME analysis on the active compounds (**9**, **12**, **13**, **14**, **15**, **22** and **25**) thrown that they did not present PAINS alerts, although they did not fulfill the leadlikeness parameters for oral dosage, presenting 1 to 3 alerts. Only **25** did not present any violation regarding Lipinski, Ghose, Veber, Egan, and Muegge parameters. Unfortunately, the most active compounds **9**, **15** and **22** were the ones that presented more druglikeness violations. In particular, **22** did not fulfill the minimum requirements to be considered as "druglike", and was the one with more alerts of the series, despite it was the most active compound.

Regarding the metabolism process, the Biotransformer analysis thrown that these compounds could be metabolized by the CYP450 complex. The compounds could be substrates of CYP1A2, CYP2B6, CYP2C8,

CYP2C9, CYP2C19, CYP2D6 and CYP3A4, and they could go under aliphatic, allylic or aromatic hydroxylations, thioether oxidation, arene epoxidation or terminal desaturation. The generation of more polar and soluble metabolites could allow a more effective elimination than expected for their parent compounds.

According to pkCSM prediction, all the active compounds present fairly good ADME-Tox properties. From the absorption estimation, we could expect a reduced colorectal permeability for **14**, **15**, **22**, and **25**, but all active compounds were predicted to have an excellent intestinal absorption. The volumes of distribution (VDss) are rather low, and it is most likely that the compounds remain bound to serum proteins, as we could expect from their solubility parameters, which could difficult the distribution process. Regarding excretion, clearance parameters were predicted to improve respect to salirasib (**12**), with the sole exception of **13**. Also, the compounds did not present signs of being mutagenic, and only **14**, **15**, and **25** presented hepatotoxicity alerts.

Although druglikeness guidelines, such as Lipinski's rule of 5 [50], establish a base of desirable parameters values that an active compound should have, in this case it seems to be "counterintuitive", since the best compounds are the heaviest, largest, more non-polar and least soluble, which translates into a low oral bioavailability, and limiting the dosage mode. These types of compounds are more likely to require a formulation process, such as liposomes, to achieve a good *in vivo* biological effect. This does not represent any disadvantage, since this type of formulations is widely used in cancer chemotherapies. For example, Doxorubicin and Daunorubicin may be given via liposomes.

Conclusion

In summary, we were able to validate our design of salirasib analogs, obtaining compounds that resulted to be better antiproliferative agents than salirasib, namely **9**, **15** and **22** (**Fig. 6**). Also, our collection of salirasib analogs contributed to get a deeper insight of the physicochemical requirements (**Fig. 7**) that this kind of compounds need in order to achieve a proper anti-tumor activity. We could determine that all active compounds presented an electron deficient carbon alpha to the sulphur, being bound to an allyl or triazolyl group, which could mean that this electron density may be important in order to achieve a good interaction with the target. Furthermore, the most active compounds **9**, **15** and **22** were characterized for having a 16 carbons long, flexible

aliphatic chain, which could be related to an improved lipophilic interaction with the enzyme. Although their physicochemical parameters are not optimal for oral dosage, other dosage forms, such as IV, could be explored.

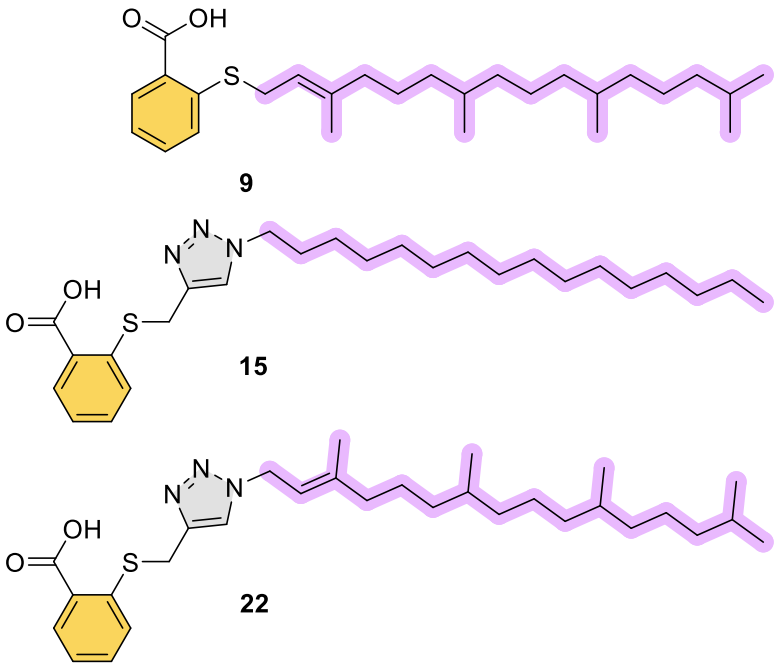

Cell line	GI_{50} (μM) 9	15	22
A549	14 ± 2.4	9.2 ± 0.7	5.4 ± 0.7
HeLa	12 ± 2.4	6.9 ± 0.04	4.3 ± 1.3
SW1573	15 ± 3.3	9.3 ± 0.03	5.8 ± 0.6
T47D	18 ± 1.3	20 ± 5.9	9.6 ± 1.3
HBL-100	14 ± 1.9	14 ± 1.2	10 ± 1.1

Fig.6. Selected most promising TSA derivatives.

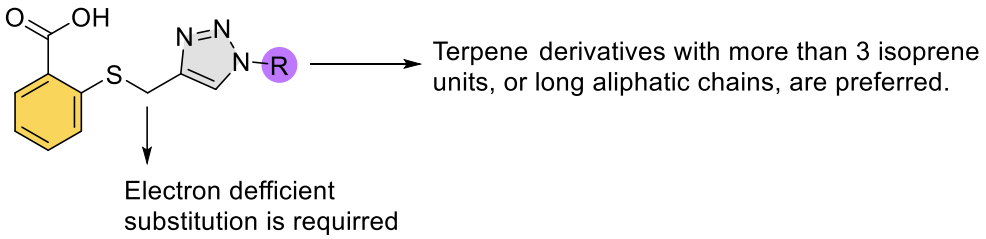

Optimal physicochemical properties:
MW > 350 Da; TSA > 300 Å2; LogD > 3; cLogS < -5

Fig 7. Structure-activity relationship of our library as antiproliferative agents.

Acknowledgements

This work was supported in part by grants from Consejo Nacional de Investigaciones Científicas y Técnicas, Agencia Nacional de Promoción Científica y Tecnológica (FONCyT PICT 2017-2096 to GRL) and Universidad Nacional de Rosario (80020190300101UR). GRL is a member of the career of the scientific investigator (CONICET). M.S.B and E.O.J.P. thank CONICET for the award of a Fellowship. J.M.P. thanks the Canary Islands Government (ProID2020010101, ACIISI/FEDER, UE) for financial support.

References

1. World Health Organization. Cancer [Internet]. . Available from: https://www.who.int/news-room/fact-sheets/detail/cancer.

2. Lau HY, Wang M. Small change, big effect: Taking RAS by the tail through suppression of post-prenylation carboxylmethylation. *Small GTPases*. 11(4), 271–279 (2018).

3. Sebti SM, Der CJ. Searching for the elusive targets of farnesyltransferase inhibitors. *Nat. Rev. Cancer*. 3(12), 945–951 (2003).

4. Berndt N, Hamilton AD, Sebti SM. Targeting protein prenylation for cancer therapy. *Nat. Rev. Cancer*. 11, 775–791 (2011).

* The general protein prenylation process is stablished and different inhibition strategies are summarized.

5. Yang WS, Yeo SG, Yang S, Kim KH, Yoo BC, Cho JY. Isoprenyl carboxyl methyltransferase inhibitors: a brief review including recent patents. *Amino Acids*. 49(9), 1469–1485 (2017).

* This review summarizes some of the most relevant ICMT inhibitors.

6. Ahmadian MR, Zor T, Vogt D, *et al.* Guanosine triphosphatase stimulation of oncogenic Ras mutants. *Proc. Natl. Acad. Sci. U. S. A.* 96(12), 7065–7070 (1999).

7. Adjei AA, Dy GK, Erlichman C, *et al.* A phase I trial of ISIS 2503, an antisense inhibitor of H-ras, in combination with gemcitabine in patients with advanced cancer. *Clin. Cancer Res.* 9(1 I), 115–123 (2003).

8. Sebti SM, Hamilton AD. Farnesyltransferase and geranylgeranyltransferase I inhibitors and cancer therapy: Lessons from mechanism and bench-to-bedside translational studies. *Oncogene*. 19(56), 6584–6593 (2000).

9. Kohl NE, Omer CA, Davide JP, *et al.* Inhibition of farnesyltransferase induces regression of mammary and salivary carcinomas in ras transgenic mice. *Nat. Med.* 1(8), 792–797 (1995).

10. Fiordalisi JJ, Johnson II RL, Weinbaum CA, *et al.* High Affinity for Farnesyltransferase and Alternative Prenylation Contribute Individually to K-Ras4B Resistance to Farnesyltransferase Inhibitors. *J. Biol. Chem.* 278(43), 41718–41727 (2003).

11. Ho A, Chau N, Wong DJ, *et al.* Preliminary results from a phase 2 proof of concept trial of tipifarnib in tumors with HRAS mutations [Internet]. In: *International Conference: Molecular Targets and Cancer Therapeutics*, Philadelphia, PA, Abstract LB-A10 (2017). Available from: https://www.abstractsonline.com/pp8/#!/4557/presentation/618.

12. Study of Tipifarnib in Patients With Previously-Treated, Advanced, HRAS Mutant Urothelial Carcinoma [Internet]. . Available from: https://clinicaltrials.gov/ct2/show/NCT02535650.

13. Schlitzer M, Winter-Vann A, Casey PJ. Non-peptidic, non-prenylic inhibitors of the prenyl protein-specific protease Rce1. *Bioorganic Med. Chem. Lett.* 11(3), 425–427 (2001).

14. Chen Y. Inhibition of K-ras-transformed rodent and human cancer cell growth via induction of apoptosis by irreversible inhibitors of ras endoprotease. *Cancer Lett.* 131(2), 191–200 (1998).

15. Mohammed I, Hampton SE, Ashall L, *et al.* 8-Hydroxyquinoline-based inhibitors of the Rce1 protease disrupt Ras membrane localization in human cells. *Bioorganic Med. Chem.* 24, 160–178 (2016).

16. Bergo MO, Lieu HD, Gavino BJ, *et al.* On the physiological importance of endoproteolysis of CAAX proteins. Heart-specific Rce1 knockout mice develop a lethal cardiomyopathy. *J. Biol. Chem.* 279(6), 4729–4736 (2004).

17. Wahlstrom AM, Cutts BA, Karlsson C, *et al.* Rce1 deficiency accelerates the development of K-RAS-induced myeloproliferative disease. *Blood*. 109(2), 763–768 (2007).

18. Winter-Vann AM, Baron RA, Wong W, *et al.* A small-molecule inhibitor of isoprenylcysteine carboxyl methyltransferase with antitumor activity in cancer cells. *Proc. Natl. Acad. Sci. U. S. A.* 102(12), 4336–4341 (2005).

19. Marciano D, Ben-Baruch G, Marom M, Egozi Y, Haklai R, Kloog Y. Farnesyl Derivatives of Rigid Carboxylic Acids-Inhibitors of ras-Dependent Cell Growth. *J. Med. Chem.* 38(8), 1267–1272 (1995).

* This is the first report on salirasib.

20. Marom M, Haklai R, Ben-Baruch G, Marciano D, Egozi Y, Kloog Y. Selective Inhibition of Ras-dependent Cell Growth by Farnesylthiosalisylic Acid. *J. Biol. Chem.* 270(38), 22263–22270 (1995).

21. Elad G, Paz A, Haklai R, Marciano D, Cox A, Kloog Y. Targeting of K-Ras 4B by S-trans,trans-farnesyl thiosalicylic acid. *Biochim. Biophys. Acta*. 1452, 228–242 (1999).

22. Haklai R, Gana-Weisz M, Elad G, *et al.* Dislodgment and Accelerated Degradation of Ras. *Biochemistry*. 37, 1306–1314 (1998).

23. Cox AD, Der CJ, Philips MR. Targeting RAS membrane association: Back to the future for anti-RAS drug discovery? *Clin. Cancer Res.* 21(8), 1819–1827 (2015).

24. Egozi Y, Weisz B, Gana-Weisz M, Ben-Baruch G, Kloog Y. Growth Inhibition of ras-Dependent Tumors in Nude Mice by a Potent ras-Dislodging Antagonist. *Int. J. Cancer*. 80, 911–918 (1999).

25. Gana-Weisz M, Halaschek-Wiener J, Jansen B, Elad G, Haklai R, Kloog Y. The Ras Inhibitor S-trans,trans-Farnesylthiosalicylic Acid Chemosensitizes Human Tumor Cells Without Causing Resistance. *Clin. Cancer Res.* 8, 555–565 (2002).

26. Laheru D, Shah P, Rajeshkumar N V, *et al.* Integrated preclinical and clinical development of S-trans,trans-farnesylthiosalicylic acid (FTS, Salirasib) in pancreatic cancer. *Invest New Drugs*. 30, 2391–2399 (2012).

27. Furuse J, Kurata T, Okano N, *et al.* An early clinical trial of Salirasib, an oral RAS inhibitor, in Japanese patients with relapsed/refractory solid tumors. *Cancer Chemother. Pharmacol.* 82(3), 511–519 (2018).

28. Kloog Y, Blum R, Cox A. Inhibitors of Chronically Active Ras: Potential for Treatment of Human Malignancies. *Recent Pat. Anticancer. Drug Discov.* 3(1), 31–47 (2008).

29. Riely GJ, Johnson ML, Medina C, *et al.* A Phase II Trial of Salirasib in Patients with Lung Adenocarcinomas with KRAS Mutations. *J. Thorac. Oncol.* 6(8), 1435–1437 (2011).

30. Ling Y, Ye X, Zhang Z, *et al.* Novel Nitric Oxide-Releasing Derivatives of Farnesylthiosalicylic Acid: Synthesis and Evaluation of Antihepatocellular Carcinoma Activity. *J. Med. Chem.* 54, 3251–3259 (2011).

31. Majmudar JD, Morrison-Logue A, Song J, Hrycyna CA, Gibbs RA. Identification of a novel nanomolar inhibitor of hIcmt via a carboxylate replacement approach. *Medchemcomm*. 3, 1125–1137 (2012).

32. Bergman JA, Hahne K, Song J, Hrycyna CA, Gibbs RA. S -Farnesyl-Thiopropionic Acid Triazoles as Potent Inhibitors of Isoprenylcysteine Carboxyl Methyltransferase. *ACS Med. Chem. Lett.* 3, 15–19 (2012).

33. Ling Y, Wang Z, Zhu H, *et al.* Synthesis and biological evaluation of farnesylthiosalicylamides as potential anti-tumor agents. *Bioorg. Med. Chem.* 22(1), 374–380 (2014).

34. Xiong Y, Hou T, Liu L, *et al.* Solanesol derived therapeutic carriers for anticancer drug delivery. *Int. J. Pharm.* 572, 118823 (2019).

35. Porta EOJ, Bofill Verdaguer I, Perez C, *et al.* Repositioning Salirasib as a new antimalarial agent. *Medchemcomm*. 10(9), 1599–1605 (2019).

** This article reports the synthesis of salirasib analogs under study in this work.

36. Skehan P, Storeng R, Scudiero D, *et al.* New colorimetric cytotoxicity assay for anticancer-drug screening. *J. Natl. Cancer Inst.* 82(13), 1107–1112 (1990).

37. Miranda PO, Padrón JM, Padrón JI, Villar J, Martín VS. Prins-type synthesis and SAR study of cytotoxic alkyl chloro dihydropyrans. *ChemMedChem*. 1(3), 323–329 (2006).

38. Sander T, Freyss J, Von Korff M, Rufener C. DataWarrior: An open-source program for chemistry aware data visualization and analysis. *J. Chem. Inf. Model.* 55(2), 460–473 (2015).

39. Davies M, Nowotka M, Papadatos G, *et al.* ChEMBL web services: Streamlining access to drug discovery

data and utilities. *Nucleic Acids Res.* 43(W1), W612–W620 (2015).

40. Mendez D, Gaulton A, Bento AP, *et al.* ChEMBL: Towards direct deposition of bioassay data. *Nucleic Acids Res.* 47(D1), D930–D940 (2019).

41. ChemAxon Calculator and Predictors [Internet]. . Available from: https://chemaxon.com/products/calculators-and-predictors.

42. Daina A, Michielin O, Zoete V. SwissADME: A free web tool to evaluate pharmacokinetics, drug-likeness and medicinal chemistry friendliness of small molecules. *Sci. Rep.* 7(January), 42717 (2017).

43. Pires DEV, Blundell TL, Ascher DB. pkCSM: Predicting small-molecule pharmacokinetic and toxicity properties using graph-based signatures. *J. Med. Chem.* 58(9), 4066–4072 (2015).

44. Djoumbou-Feunang Y, Fiamoncini J, Gil-de-la-Fuente A, Greiner R, Manach C, Wishart DS. BioTransformer: A comprehensive computational tool for small molecule metabolism prediction and metabolite identification. *J. Cheminform.* 11, 2 (2019).

45. Lagunes I, Martín-Batista E, Silveira-Dorta G, Fernandes MX, Padrón JM. Differential mechanism of action of the CK1ε inhibitor GSD0054. *J. Mol. Clin. Med.* 1(2), 77–83 (2018).

46. SIGNUM BIOSCIENCES I, LEE S-Y, VORONKOV M, WOLANIN P. Acetyl mimic compounds for the inhibition of isoprenyl-S-cysteinyl methyltransferase. (2009).

47. SIGNUM BIOSCIENCES I, VORONKOV M, STOCK J, *et al.* Anti-inflamatory complexes. (2010).

48. SIGNUM BIOSCIENCES I, STOCK J, STOCK M, *et al.* Isoprenyl compounds and methods thereof. (2010).

49. SIGNUM BIOSCIENCES I, VORONKOV M, PEREZ E, HEALY J, FERNANDEZ J. Compounds and methods use. (2018).

50. Lipinski CA, Lombardo F, Dominy BW, Feeney PJ. Experimental and computational approaches to estimate solubility and permeability in drug discovery and development settings. *Adv. Drug Deliv. Rev.* 46, 3–26 (2001).